NMR spectroscopy to study cyclodextrin-based host-guest assemblies with polynuclear clusters

Mohamed Haouas, Clément Falaise, Nathalie Leclerc, Sébastien Floquet, Emmanuel Cadot

NMR Spectroscopy to Study Cyclodextrin-Based Host-Guest Assemblies with Polynuclear Clusters

Mohamed Haouas, Clément Falaise, Nathalie Leclerc, Sébastien Floquet and Emmanuel Cadot*

AUTHORS ADDRESS

Institut Lavoisier de Versailles (ILV), Université Paris-Saclay, UVSQ, CNRS, 45 avenue des Etats-Unis, 78000, Versailles, France

ABSTRACT. Natural cyclodextrin (CD) macrocycles are known to form diverse inclusion complexes with a wide variety of organic molecules, but recent work has revealed that inorganic clusters also form multicomponent supramolecular complexes and edifices. Such molecular assemblies exhibit a high degree of organization in solution governed by various chemical processes including molecular recognition, host-guest attraction, hydrophobic repulsion, or chaotropic effect. Nuclear magnetic resonance (NMR) spectroscopy is one of the most efficient and practical analytical technique to characterize the nature, the strength and the mechanism of these interactions in solution. This review provides a brief overview on recent examples of the contribution of NMR to the characterization of hybrid systems in solution based on CD with polynuclear clusters, including polyoxometalates (POMs), metallic clusters and hydroborate clusters. The focus will be first on using ^{1}H (and ^{13}C) NMR of the host, *i.e.*, CD, to identify the nature of the interactions and measure their strength. Then, 2D NMR methods will be illustrated by DOSY as a means of highlighting the clustering phenomena, and by NOESY/ROESY to evidence the spatial proximity and contact within the supramolecular assemblies. Finally, other NMR nuclei will be selected to probe the inorganic part as a guest molecule. Attention will be paid to classical host-guest complexes Cluster@CD, but also to hierarchical multi-scale, multi-component assemblies such as Cluster@CD@Cluster.

1. Introduction

Molecular recognition in biology, which exploits the high affinity of bindings/interactions between specific pairs of host and guest molecules, is an infinite source of inspiration for innovation in materials science.[1,2] Molecular signal detection is probably one of the most important bioinspired functions, which may be of interest in various fields such as medical engineering, therapeutic

treatment, and sensing.[3–5] The processes involved are mainly based on supramolecular chemistry, where self-assembly through weak chemical bonds, *i.e.,* hydrophobic, electrostatic, and ionic-dipole interactions, is the driving force behind stable systems.[6–9] The spontaneous association of two or more components in solution to produce hybrid systems by coordination or supramolecular chemistry requires favorable physicochemical phenomena with minimal energy cost.[10,11] The construction of multifunctional assemblies based on supramolecular complexes usually involves the use of macrocyclic molecules to host various guest species.[5,12,13]

Cyclodextrins (CDs) represent a group of macrocyclic oligosaccharides mainly constituted of 6, 7, or 8 D-glucopyranoside units.[14] Thus, the three renowned corresponding forms, *i.e.*, α–, β–, and γ–CD, present a hydrophobic cavity of different diameter sizes depending on the number of the repeating glucopyranose group. While CDs are known for a long time to interact with various hydrophobic substances, it is now admitted that CDs are also capable of forming host-guest adducts with a wide variety of hydrophilic polynuclear metallic clusters.[15] Such self-assembly properties of CDs have proven useful for the development of smart materials based on supramolecular hybrid systems.[16,17] Hybrid associations between CDs and inorganic species can be divided into two categories. The first results from the strong affinity of the CD with a hydrophobic group grafted to the inorganic moieties. Such a mode of interaction fits into the well-established classical hydrophobic effect.[18–21] The second type involves native inorganic species such as polyoxometalates (POMs) or ionic cluster compounds which were found to form unusually stable host-guest adducts with CDs. In 2015, both Nau's and Stoddart's groups reported that γ- or β-CD interacts strongly with hydrophilic ions such as $[B_{12}X_{12}]^{2-}$ clusters (with X = H, F, Cl, Br or I) and $[PMo_{12}O_{40}]^{3-}$ anions, as revealed by single-crystal X-ray diffraction (XRD).[22,23] These solid-state arrangements showed a 2:1 sandwich-type complex where the inorganic ionic species, *i.e.*,

either the dodecaborate anions or the POM, appears surrounded by two CDs. It is interesting to note that depending on the anionic guest, the interaction of the CD involves its secondary face in the case of the cluster or its primary face in the case of POM. This molecular recognition behavior thus appears as a distinctive feature of CD in the inclusion phenomenon with inorganic clusters.

The inclusion phenomenon involving hydrophilic ionic species has been recently well documented and explained as a solvent effect that arises from the chaotropic nature of the ionic guest.[24,25] Such a chaotropic effect occurring in aqueous solution gives a characteristic thermochemical fingerprint. Low charge density species locally cause the breakdown of the water structure, characterized by a high-enthalpy and a high-entropy solvation shell. Throughout the aggregation process leading to guest encapsulation, the release of water from the hydration shell to the bulk is associated with strong decreases in enthalpy and entropy, *i.e.*, $\Delta_r H < 0$ and $\Delta_r S < 0$. Despite the entropy penalty, the aggregation process remains highly favorable and enthalpically driven ($T\Delta_r S > \Delta_r H$ and $\Delta_r G < 0$). Thus, several POM-based chemical systems with low charge density, including the Lindqvist ions $[M_6O_{19}]^{2-}$,[26] the Preyssler-type anion $[P_5W_{30}O_{110}]^{15-}$,[27] the Dawson-type anion $[P_2W_{18}O_{62}]^{6-}$,[28] and even, the giant Mo blue wheel $[Mo_{154}O_{462}H_{14}(H_2O)_{70}]^{14-}$, abbreviated $\{Mo_{154}\}$,[29,30] have verified such affinity. The phenomenon can then be generalized regardless of the structure, composition, size and shape of the POM.[24,25] Although the chaotropic effect was identified by Hofmeister in 1888 for small ions, this property has been clearly associated with cluster anions only very recently and opens a new avenue for the design of CD-based smart supramolecular materials.[7,31–36]

The characterization of CD complexation by polynuclear clusters is of paramount importance to understand the driving forces of the phenomena involved in solutions such as self-assembly, host-guest inclusion, and aggregation process. Various analytical techniques such as calorimetric titration,[37] ESI-mass spectrometry,[38,39] X-ray scattering and diffraction,[1,40] circular

dichroism,[21,36,41] voltammetry[41] and fluorescence spectroscopy[42] were applied to study the reactivity of CDs with different guest molecules. Furthermore, NMR spectroscopy is one of the most frequently used methods for studying self-assembly processes with CDs,[43–46] allowing to determine not only quantitative information, e.g., the stoichiometry of adducts and their binding constants but also structural and dynamic data of the complex and its constituent parts, e.g., the regioselectivity of the binding sites and their equilibria and exchanges. This mini-review focuses on the recent use of NMR methodology to study complexation of CD with inorganic polynuclear species.

2. Probing host-guest interaction by ^{1}H and ^{13}C NMR of cyclodextrin

Cyclodextrins are highly symmetrical molecules consisting of identical D-glucopyranoside motifs. The ^{1}H NMR in aqueous solution thus shows the signature of this glucopyranoside unit which has six distinctive proton sites, labeled H1 (anomeric position), H2, H3, H4, H5 and H6 (See Fig. 1).[46] The three hydroxyl groups are not distinguishable and merge with the water signal due to their chemical exchange. Because the molecules are cyclic H2 and H4 are exposed to the outside, while H3 and H5 are located inside the central cavity of the tori. The H6 protons correspond to the methanolic arms at the top of the primary face of the macrocycles. Fig. 1 is a representative ^{1}H NMR spectrum in D_2O of 3 mM solution of γ-CD. The anomeric proton H1 appears strongly deshielded at ca. 5 ppm, while the other protons are only partially resolved and divided into two groups, at 3.4-3.6 ppm (outward protons H2 and H4) and 3.7-3.9 ppm (inward protons H3, H5, and H6). The latter are obviously the most sensitive to interaction with guest molecules and are often used as probes for host-guest complexation.

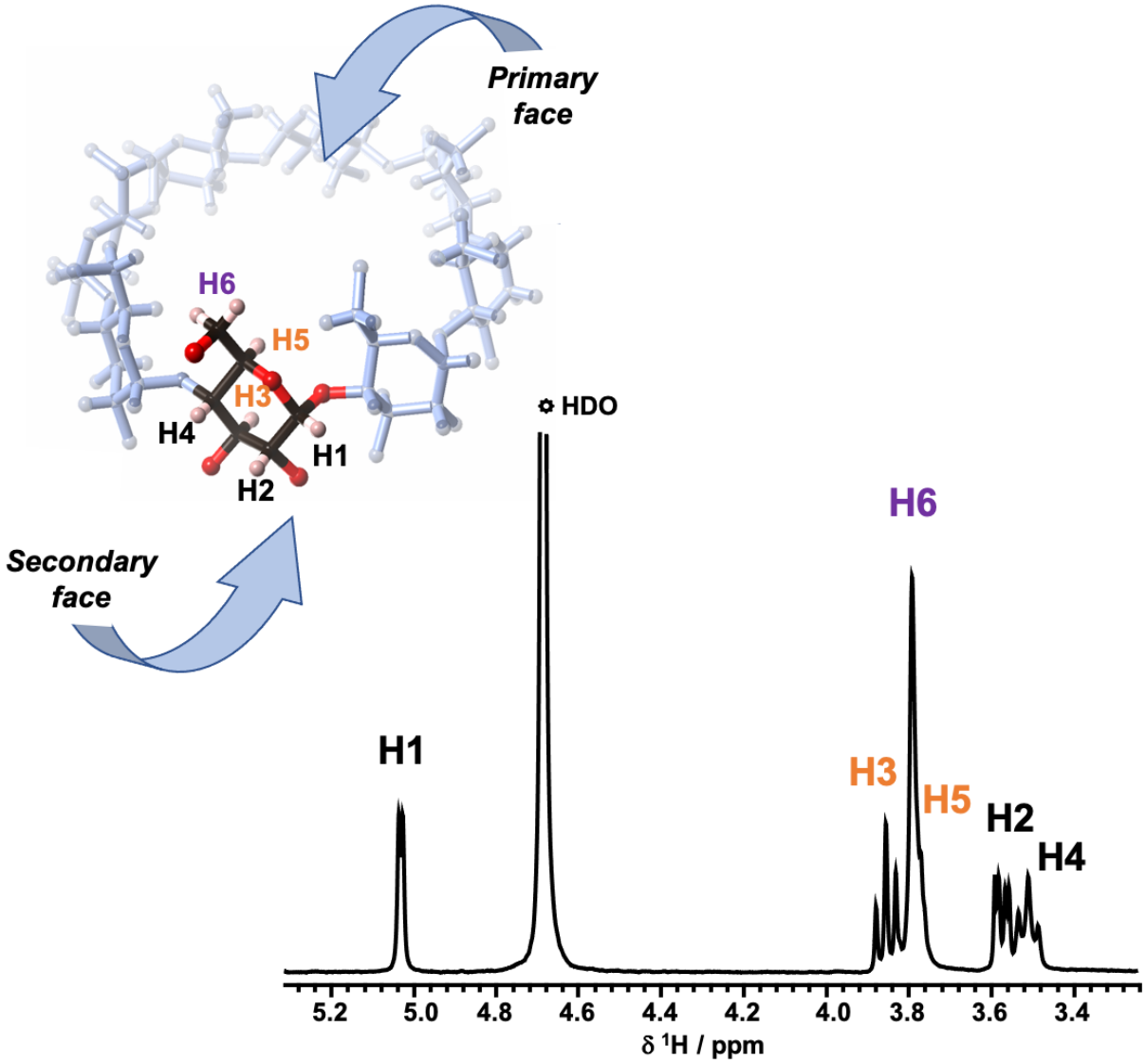

Fig. 1. ^{1}H NMR spectrum of 3 mM γ-CD in D_2O showing the six signals of the macrocycle: the anomeric proton H1, the outward protons H2 and H4, the inward protons H3 and H5, and the methanolic H6 protons on the primary face.

One of the simplest experiments to identify the host-guest interaction in solution between CD and inorganic species is the ^{1}H NMR titration of the host molecule by the guest species to observe the effects on the resonances of the most exposed protons, those present on the inner surface of the cavity. Fig. 2 shows an example of titration of 3 mM D_2O solution of γ-CD by two anionic clusters: the selenide octahedral rhenium cluster $[Re_6Se_8(CN)_6]^{4-}$ and the Dawson-type POM $[P_2W_{18}O_{62}]^{6-}$.[6,28] Two antagonist behaviors are observed. With the rhenium cluster complex, the most affected

resonance upon addition of 4 eq. corresponds to the H3, down-field shifting from ca. 3.9 to 4.3 ppm, whereas in case of the POM, this resonance did not move so much, and instead, H6 underwent up to 0.3 ppm downfield shift. This illustrates the difference in supramolecular recognition process in solution. CD reacts with the rhenium cluster to form inclusion complex involving their secondary face, which differs from the sandwich adduct through its primary rim obtained with the Dawson-type POM (see Fig. 2). These observations in aqueous solution are consistent with the molecular organization in the solid-state, but has to consider the dynamics aspect of the host-guest association equilibria. As evidence of molecular recognition, competition occurs in the simultaneous presence of two guests, Dawson-type POM and octahedral rhenium cluster.[47]

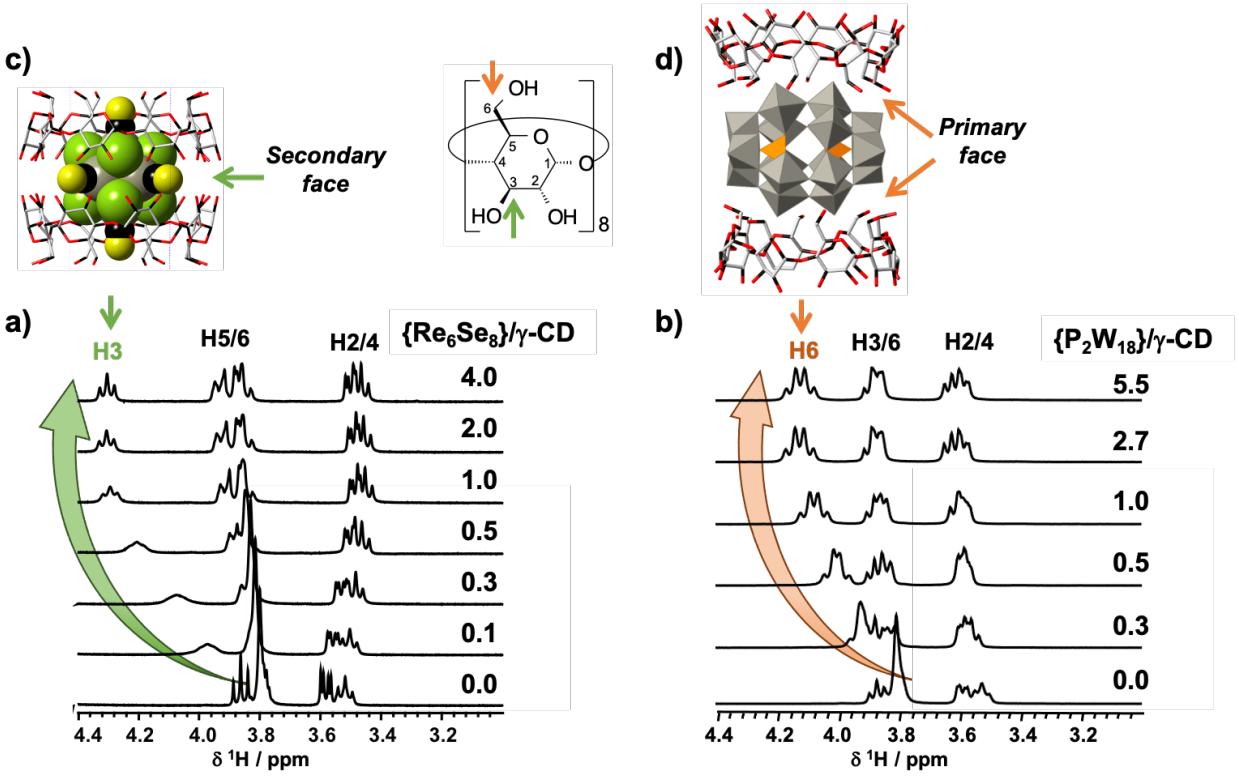

Fig. 2. ^{1}H NMR titration of 3 mM γ-CD in D_2O by (a) $[Re_6Se_8(CN)_6]^{4-}$ and (b) $[P_2W_{18}O_{62}]^{6-}$ in the range 3.0-4.4 ppm. (c) and (d) the crystallographic structures of the adducts obtained in each system. Adapted from references.[6,28]

The dynamic aspect of the host-guest association could also inform the strength of the interaction between the two components. Generally speaking, a slow dissociative process usually indicates a strong complexation. This can be easily observed in the NMR titration experiment. When the equilibria are fast relative to the NMR time scale, the CD signals appear as a weighted average situation between free and bound species. This is manifested by a continuous shift of some specific resonances, as observed in the cases of $[Re_6Se_8(CN)_6]^{4-}$ and $[P_2W_{18}O_{62}]^{6-}$ with γ-CD in Fig. 2. The scenario is different with molybdenum clusters $[Mo_6X_8Cl_6]^{2-}$ (X = Br or I) when the NMR signatures of γ-CD exhibit slow exchange regime,[48] as shown in Fig. 3. Here, the signals of free and complexed CD are observed together, allowing even the stoichiometry of the final adduct to be easily determined. Indeed, consumption of free CD occurs at 0.5 eq. of cluster confirming a 2:1 sandwich complex in agreement with the XRD structures (Fig. 3).

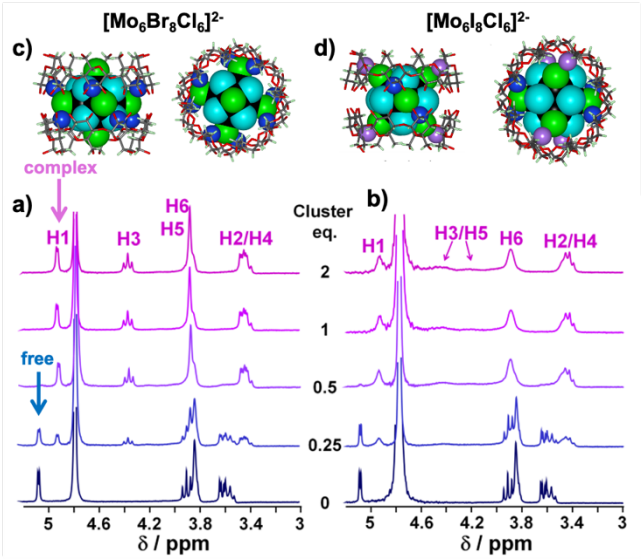

Fig. 3. ^{1}H NMR titration of 2 mM γ-CD in D_2O by (a) $[Mo_6Br_8Cl_6]^{2-}$ and (b) $[Mo_6I_8Cl_6]^{2-}$. (c) and (d) the crystallographic structures (top and side views) of the adducts obtained in each system. Color code: black = Mo, light blue = X (Br or I), green = Cl. H3 and H5 involved in close host–guest interactions are in dark blue and pink, respectively. Adapted from reference.[48]

The interaction of octahedral metal clusters with γ-CD often leads to sandwich-like host-guest complexes, as revealed by XRD analysis. However, the behavior in solution may differ dramatically from one cluster to another. Some clusters like $[Re_6X_8(CN)_6]^{4-}$ (X = S or Se) showed labile complexes indicating moderate association affinity ($K_{1:1}$ < 2000 M^{-1}), while others like $[Mo_6X_8Cl_6]^{2-}$ (X = Br or I) are characterized by frozen complexation in solution due to strong attraction between the two components. Such behavior comes from a chaotropic effect induced complexation where the guest dehydration and its association with neutral surfaces such as hydrophobic CD cavities are very favorable processes.[24,25,49] Here, the overall charge of the polyanion plays a crucial role, and the general trend shows that the lower the charge density, the stronger the host-guest association. In comparison, POMs can have a very strong chaotropic character, but they lead almost exclusively to dynamically labile systems. It seems therefore difficult to reconcile the thermodynamic stability of these supramolecular associations and their dynamics in solution, even if the general tendency shows that frozen complex reflects a strong association.

Internal dynamics can also be detected in a frozen system, as in the case of molybdenum chloride clusters with γ-CD shown in Fig. 3.[48] The NMR spectra of the iodine derivative are broader than those obtained with Br-based clusters. This would indicate a different rotational dynamic within the host-guest assembly, induced by a reorientation of the cluster in the CD cavities after a 45° tilt from the central axis of the CD (Fig. 3). With iodide compound, all the six apical chlorine ligands are located inside the cavities of the capping CDs, maximizing the weak attractive forces

with the host and thus restricting internal molecular movement within the supramolecular framework. Host size may also play a key role in these associations and their dynamics since the volume of cluster $[Mo_6X_8Cl_6]^{2-}$ increases from 395 to 447 $Å^3$ by substituting X with Br and I, respectively.

Interaction of cyclodextrins with cationic transition metal octahedral clusters has also been studied, and their behavior in solution has been found mostly to depend on the nature of their inner ligands like with anionic clusters. For instance, very different results were obtained with $[Nb_6Cl_{12}(H_2O)_6]^{2+}$ when compared to $[Ta_6Br_{12}(H_2O)_6]^{2+}$ although both had led to isostructural sandwiched inclusion 2:1 complexes with γ-CD in the solid-state.[1,28] While titration experiment with $[Ta_6Br_{12}(H_2O)_6]^{2+}$ showed frozen complexation in solution, the ^1H NMR spectra in the case of $[Nb_6Cl_{12}(H_2O)_6]^{2+}$, shown in Fig. 4, clearly indicate no host-guest inclusion happened and only weak contacts took place at the external peripheral wall of the CD. Indeed, the signals of H3 and H6 protons at the two different rims did not undergo any significant alteration, while resonances of H1 and H4 protons pointing outward the cavity shifted significantly in the presence of the cluster. In a similar way, no interaction has been recorded with the chloride derivative of $[Mo_6Cl_8Cl_6]^{2-}$,[50] while the bromide and iodide cluster complexes $[Mo_6X_8Cl_6]^{2-}$ (X = Br or I) interact strongly with γ-CD.[48]

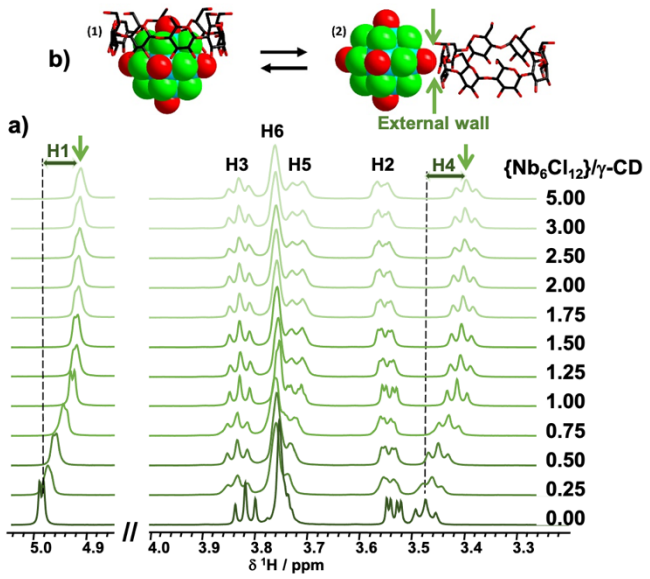

Fig. 4. (a) ^{1}H NMR titration of 1 mM γ-CD in D_2O by $[Nb_6Br_{12}(H_2O)_6]^{2+}$. (b) A schematic illustration of the dynamic dissociation of the host-guest complex observed in the solid state (1) occurring in solution (2). Adapted from reference.[1]

Given their spherical shape and nanoscale size, Keggin-type POMs are expected to react with CDs to readily form host-guest inclusion complexes in a similar way to octahedral metal-atom clusters. Nonetheless, the isolation of well-defined supramolecular assemblies is rather rare with POMs. The interaction in solution was found to be strongly dependent on the charge of the POM as shown in Fig. 5,[25] depicting the ^{1}H NMR titration of 2 mM γ-CD with four different Keggin-type POMs $[XW_{12}O_{40}]^{n-}$, X = P, Si, B, and H_2, whose overall charge *n* varied from 3- to 6-. Almost no effect can be detected with the most charged POM $[H_2W_{12}O_{40}]^{6-}$, indicating very weak interaction between the POM and organic macrocycle. With the boron and silicon derivatives moderate effects on H6 signal can be seen, comparable to that observed with the Dawson-type POM (Fig. 2), indicative of supramolecular contact of the POM with the primary face of the CD. The situation is even more different with the Keggin-type dodecatungstophosphate $[PW_{12}O_{40}]^{3-}$ where H3 exhibited the strongest effect as clear evidence of embedment of the POM within the

central cavity of the CD. Indeed, among the four Keggin-type POMs studied, only $[PW_{12}O_{40}]^{3-}$ had conducted to crystal structure of host-guest adduct where the POM is deeply embedded within the central cavity through the secondary face of the γ-CD. The X-ray structure with the boron derivative showed co-crystallization of the POM and the CD side-by-side without inclusion complexation. Again, these results are explained by the chaotropic nature of the polyanions. When the hydration network is loosely defined and weakly organized, desolvation can occur easier. Obviously, the charge density of the POM affects the solvation properties and the higher the charge density, the lower the desolvation ability (or the chaotropic power).

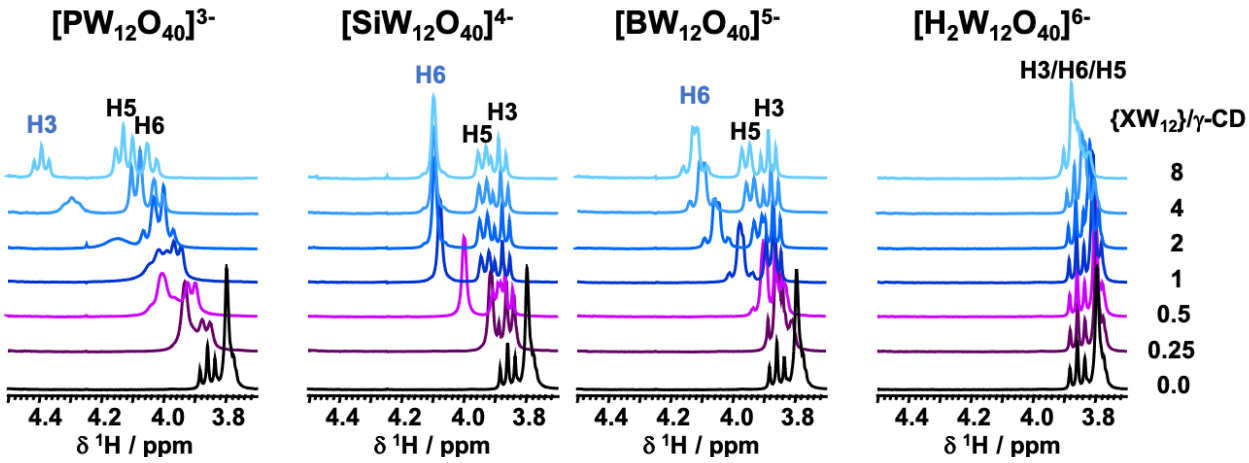

Fig. 5. ^{1}H NMR titration of 2 mM γ-CD in D_2O by Keggin POMs $[XW_{12}O_{40}]^{n-}$: X = P, Si, B, H_2, and n = 3, 4, 5, 6. Adapted from reference.[25]

Similar results were obtained with the molybdenum Keggin POMs, confirming that the nature of the metal center, *i.e.*, Mo^{6+} or W^{6+}, does not affect much the interaction with the CD. However, the effects of POM on the ^{1}H NMR response are different depending on the size of the CD highlighting the importance of the host-guest size matching in the encapsulation process. Fig. 6 displays the obtained ^{1}H NMR titration of three different solutions of α-, β-, and γ-CD by

222 $[PMo_{12}O_{40}]^{3-}$ (4 mM in D_2O).[51] The evolution of the spectra of γ-CD is very similar to that
223 observed with $[PW_{12}O_{40}]^{3-}$ (see Fig. 5), where H2 and H4 show only a negligible effect by
224 comparison to H3, and to a lesser extent to H5 and H6, experiencing all strong deshielding
225 effects. On the other hand, no significant effect can be seen on H3 resonance in α- and β-CD
226 solutions, and only moderate shifts are detected for H6 and H5 signals. These results indicate
227 that interactions occur mainly with the primary face of the CD without deep inclusion within the
228 organic macrocycle since the chemical shift of the internal H3 proton remains unaffected. It
229 appears therefore clear that the α- and β-CD interact mostly with the POM through their outer
230 surface, while γ-CD leads to the usual host–guest inclusion, involving its internal cavity. The α-
231 and β-CD are too small to entirely accommodate Keggin-type POM in their central cavity.
232

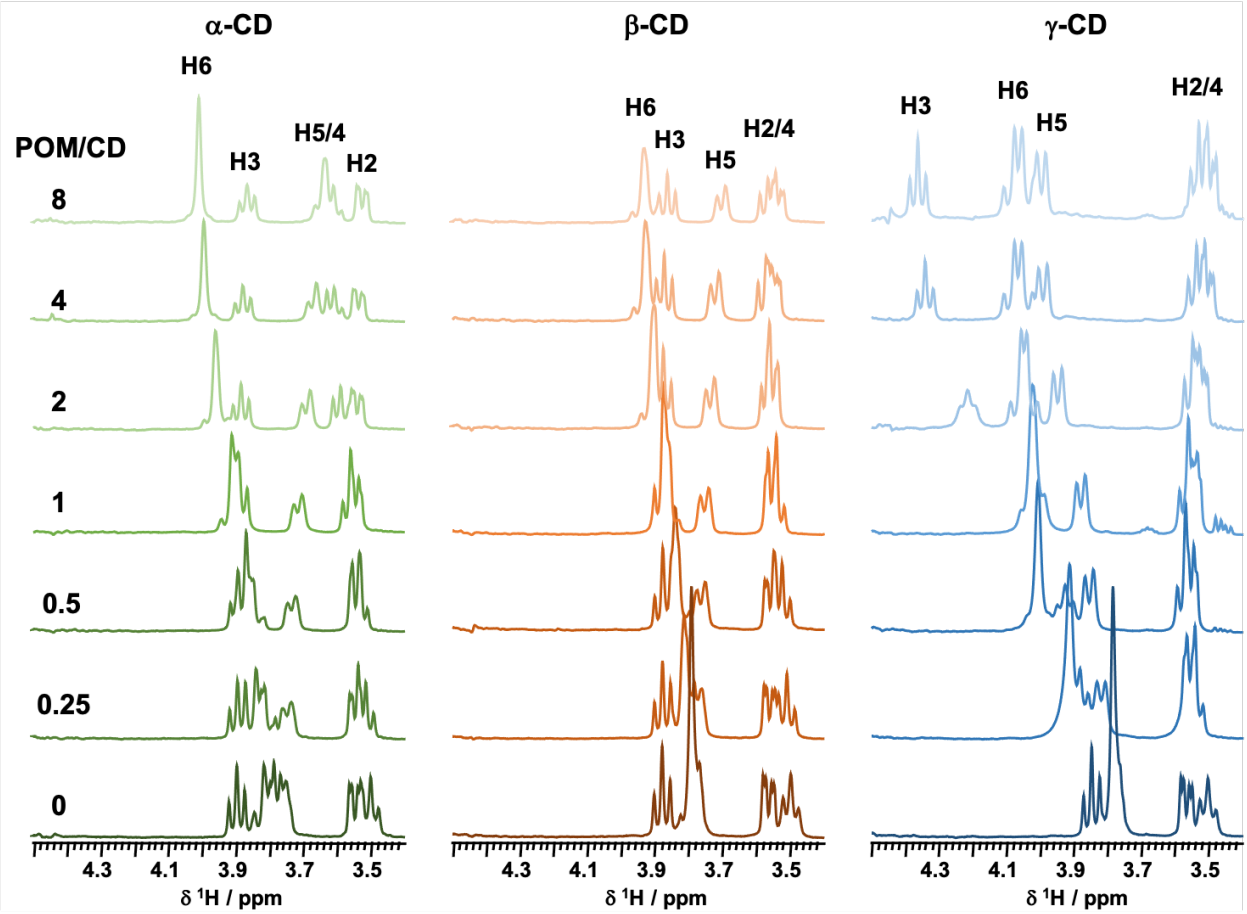

Fig. 6. ^{1}H NMR titration of 4 mM α-, β-, and γ-CD in D_2O by Keggin-type POM $[PMo_{12}O_{40}]^{3-}$. Reproduced from reference.[51]

The use of ^{13}C NMR in titration is rather rare due to the very poor sensitivity compared to ^{1}H NMR despite the considerable gain in resolution. As an example of such experiments, Fig. 7 shows the obtained ^{13}C{^{1}H} NMR of 3 mM γ-CD titrated by the rhenium clusters $[Re_6S_8(CN)_6]^{4-}$ and $[Re_6Se_8(CN)_6]^{4-}$ up to 8 equivalents.[6] The behavior of the CD in the presence of the two clusters is different. First, C1 and C4 signals undergo deshielding with the selenide cluster, while these signals evolve toward the reverse shielding direction with the sulfide cluster. Secondly, the variations of signal position are faster (lower cluster equivalents) with the Se-based cluster than the S-based cluster. For instance, the crossing of the C2 and C3 signals happens at ca. 0.25 equivalent of $[Re_6Se_8(CN)_6]^{4-}$, while it occurs at ca. 2 equivalents of $[Re_6S_8(CN)_6]^{4-}$. This result

indicates stronger affinity between the CD and $[Re_6Se_8(CN)_6]^{4-}$ than $[Re_6S_8(CN)_6]^{4-}$ in agreement with the difference in association constants measured for these clusters, $K_{1:1}$ = 1500 *vs* 900 M^{-1}, respectively (see Table 2).

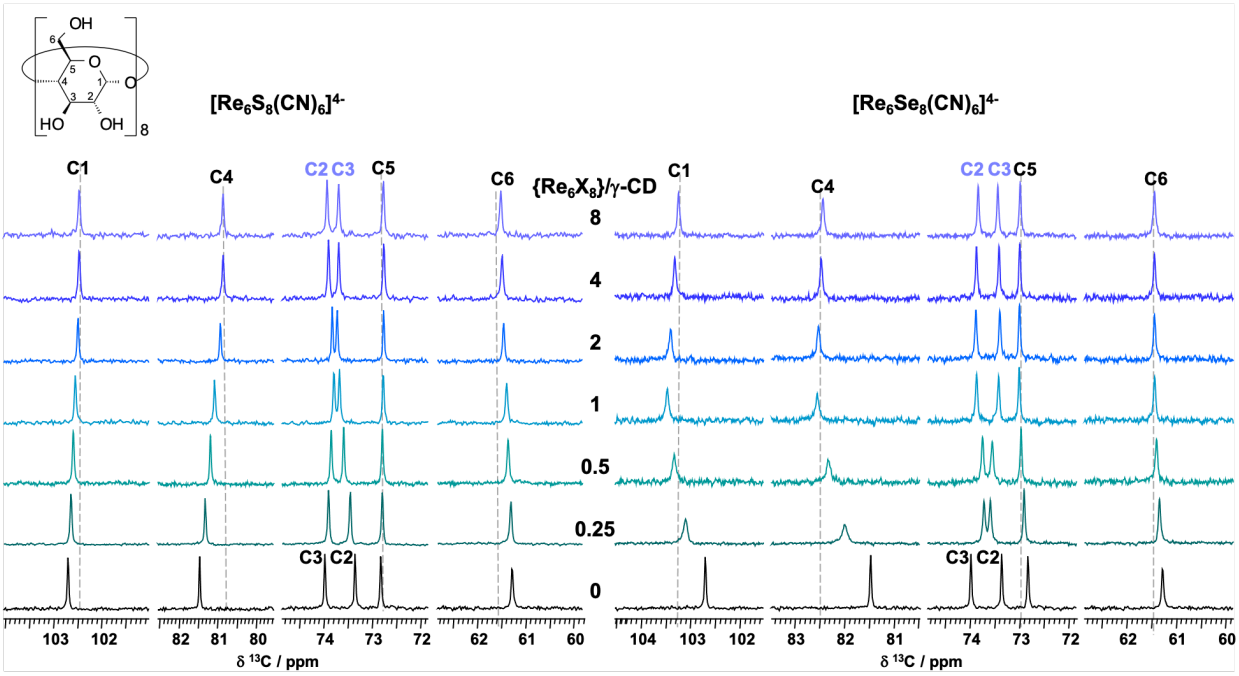

Fig. 7. $^{13}C\{^1H\}$ NMR titration of 3 mM γ-CD in D_2O by (left) $[Re_6S_8(CN)_6]^{4-}$ and (right) $[Re_6Se_8(CN)_6]^{4-}$.

3. Quantitative analysis: Determination of binding constants

NMR is a quantitative analytical tool for studying chemical equilibria and dynamic phenomena.[52] The association constants between the polynuclear cluster and the host CD can be determined from NMR titration by applying mathematical approach.[53,54] In the case of a fast chemical exchange regime relative to the NMR time scale, when a single NMR signal representative of all the different binding states is observed, the variation in the apparent chemical shift (δ_{obs}) of the CD resonances should correspond to a linear combination of the individual chemical shifts of the CD in its

different states, *i.e.,* the free CD and the 1:1, 1:2, … etc. adducts, noted respectively δ_0, $\delta_{1:1}$, $\delta_{1:2}$, ... etc. This relationship illustrated by equation (1) implies mole fractions x_0, $x_{1:1}$, $x_{1:2}$, … etc. of each CD species in free and adduct forms of 1:1, 1:2, … etc.

$$\delta_{obs} = x_0\delta_0 + x_{1:1}\delta_{1:1} + x_{1:2}\delta_{1:2} + \cdots etc. \quad (1)$$

In the simplest case of a 1:1 adduct, the association constant *K* is given by equation (2), using the CD molar fractions x_0 and $x_{1:1}$ and expressed as a function of the initial CD concentration C^0 and the molar ratio *R* = [Cluster]/[CD].

$$K = \frac{x_{1:1}}{x_0\left(R - \left(\frac{1 - x_0 + x_{1:1}}{2}\right)\right)C^0} \quad (2)$$

By combining equations (1) and (2), and assuming that $x_0 + x_{1:1} = 1$, we can deduce the expression of the observed chemical shift as a function of binding constant *K* (eqn (3)).

$$\delta_{obs} = \delta_0\left[\frac{KC^0 - KC^0R - 1 + \sqrt{(KC^0R - KC^0 + 1)^2 + 4KC^0}}{2KC^0}\right] + \delta_{1:1}\left[\frac{KC^0 + KC^0R + 1 - \sqrt{(KC^0R - KC^0 + 1)^2 + 4KC^0}}{2KC^0}\right] \quad (3)$$

Modeling the experimental data ($\delta_{obs} = f(R)$) with equation (3) enables us to estimate the binding constant *K* for the 1:1 complexation model. The individual chemical shifts (δ_0 and $\delta_{1:1}$) can be measured from independent experiments of a free CD solution and a solution with a large excess of Cluster over CD, respectively. For a more complex model, such as a 1:2 adduct, it becomes difficult to use this NMR approach to resolve the binding constants $K_{1:1}$ and $K_{1:2}$ due to the overparameterization. Indeed, prior knowledge of the individual chemical shifts $\delta_{1:1}$ and $\delta_{1:2}$, is required, that are difficult to determine in fast exchange spectra. In this case, other experimental techniques such as ITC would be more appropriate.

Thus, ^{1}H NMR is a useful internal probe to identify the nature and the strength of the supramolecular interaction between CD and inorganic clusters. In particular, the binding sites (e.g., secondary *versus* primary face), the location of the interaction (e.g., the interacting proton), and the association constants are the most valuable information determined. As a result, several types of CD-cluster hybrids are obtained from weak surface contact adducts to deeply encapsulated host-guest complexes.[30,41,55] Tables 1-3 summarize the main CD-based hybrid adducts and complexes observed with POM, boron, and octahedral metal-atom clusters studied in solution by NMR.

Table 1. Summary of reported CD-POM adducts studied in solution by NMR.

CD	POM	CD-POM adduct[a]	binding site[b]	Most affected H	Δδ (ppm)[c]	Binding constant $K_{1:1}$ (10^3 M^{-1})[d]	Ref.
α-CD	$[PW_{12}O_{40}]^{3-}$	CD•POM	P. F.	H6	+0.20	0.98	51,56
	$[P_2W_{17}O_{61}\{Sn(C_6H_4I\}]^{7-}$	POM@CD	S. F.	H5	+0.16	0.78	19
	$[P_2Mo_5O_{23}]^{6-}$	CD•POM	E. W.	-	0	-	57
	$[AlMo_6(OH)_6O_{18}]^{3-}$	3CD•4POM	E. W.	H2	+0.06	-	58
	$[PMo_{12}O_{40}]^{3-}$	-	P. F.	H6	+0.20	0.26	51
	$[V_6O_{13}((OCH_2)_3C\text{-}CH_2CH_3)_2]^{2-}$	-	S. F.	H5	-0.04	0.23	59
	$[V_6O_{13}((OCH_2)_3C\text{-}NO_2)_2]^{2-}$	POM@CD	P. F.	H3	-0.01	0.30	59
	$[V_6O_{13}((OCH_2)_3C\text{-}CH_2OH)_2]^{2-}$	-	-	-	0	-	59
	$[V_6O_{13}((OCH_2)_3C\text{-}NH(BOC))_2]^{2-e}$	-	P. F.	H5	+0.12	0.36	59
	$[MPd_{12}O_8(PhAsO_3)_8]^{2-f}$	POM@2CD	S. F.	H3	-0.03	-	35
β-CD	$[PW_{12}O_{40}]^{3-}$	-	P. F.	H6	+0.15	0.43	51
	$[P_2W_{17}O_{61}\{Sn(C_6H_4I\}]^{7-}$	POM@CD	P. F.	H5	-0.29	1.0	19
	$[P_2Mo_5O_{23}]^{6-}$	CD•POM	E. W.	-	0	-	57
	$[MnMo_9O_{32}]^{6-}$	POM@CD	E. W.	H1/H2	-0.07	-	60
	$[PMo_{12}O_{40}]^{3-}$	POM@2CD	P. F.	H6	+0.15	0.39	23,51
	$[V_6O_{13}((OCH_2)_3C\text{-}CH_2CH_3)_2]^{2-}$	-	S. F.	H5	-0.17	0.70	59
	$[V_6O_{13}((OCH_2)_3C\text{-}NO_2)_2]^{2-}$	POM@CD	S. F.	H5	-0.15	0.47	59

	$[V_6O_{13}((OCH_2)_3C\text{-}CH_2OH)_2]^{2-}$	POM@2CD	S. F.	H5	-0.10	0.29	[59]
	$[V_6O_{13}((OCH_2)_3C\text{-}NH(BOC))_2]^{2-e}$	POM@2CD	S. F.	H5	-0.10	1.2	[59]
γ-CD	$[W_6O_{19}]^{2-}$	POM@CD	I. C.	H5	+0.50	-	[26]
	$[PW_{12}O_{40}]^{3-}$	POM@CD	S. F.	H3	+0.53	140	[25,51,54,61]
	$[SiW_{12}O_{40}]^{4-}$	-	P. F.	H6	+0.30	17	[25,38]
	$[BW_{12}O_{40}]^{5-}$	CD•POM	P. F.	H6	+0.33	1.1	[25]
	$[H_2W_{12}O_{40}]^{6-}$	-	P. F.	H6	+0.07	0.023	[25]
	$[SiW_{11}MoO_{40}]^{4-}$	-	P. F.	H6	+0.29	11	[54]
	$[SiW_{11}MoO_{40}]^{5-}$	-	P. F.	H6	+0.10	0.73	[54]
	$[PW_{11}VO_{40}]^{4-}$	-	P. F.	H6	+0.31	7.8	[54]
	$[PW_{11}VO_{40}]^{5-}$	-	P. F.	H6	+0.10	0.86	[54]
	$[SiW_{11}VO_{40}]^{5-}$	-	P. F.	H6	+0.28	0.39	[54]
	$[SiW_{11}VO_{40}]^{6-}$	-	-	-	0	0.13	[54]
	$[P_2W_{18}O_{62}]^{6-}$	POM@2CD	P. F.	H6	+0.30	3.2	[28]
	$[P_5W_{30}O_{110}]^{15-}$	CD•POM	S. F.	H6	+0.05	0.43	[27]
	$[P_2Mo_5O_{23}]^{6-}$	CD•POM	E. W.	-	0	-	[57]
	$[Mo_6O_{19}]^{2-}$	POM@CD	I. C.	H5	+0.65	-	[26]
	$[AlMo_6(OH)_6O_{18}]^{3-}$	CD•POM	E. W.	H2	+0.02	-	[58]
	$[An\text{-}AlMo_6(OH)_3O_{18}]^{3-g}$	-	I. C.	H5	-0.40	-	[18]
	$[An_2\text{-}MnMo_6O_{18}]^{3-g}$	-	I. C.	H5	-0.40	-	[18]
	$[MnMo_9O_{32}]^{6-}$	POM@2CD	E. W.	H2	-0.11	-	[60]
	$[PMo_{12}O_{40}]^{3-}$	POM@2CD	S. F.	H3	+0.70	56	[23,51]
	$[Mo_{154}O_{462}H_{14}(H_2O)_{70}]^{14-}$	CD@POM	E. W.	H2	+0.50	-	[30]
	$[V_6O_{13}((OCH_2)_3C\text{-}CH_2CH_3)_2]^{2-}$	-	P. F.	H6	+0.11	0.32	[59]
	$[V_6O_{13}((OCH_2)_3C\text{-}NO_2)_2]^{2-}$	POM@2CD	P. F.	H5	+0.24	1.4	[59]
	$[V_6O_{13}((OCH_2)_3C\text{-}CH_2OH)_2]^{2-}$	POM@2CD	P. F.	H6	+0.12	0.090	[59]
	$[V_6O_{13}((OCH_2)_3C\text{-}NH(BOC))_2]^{2-e}$	-	P. F.	H6	+0.22	1.0	[59]

[a] From crystal structure when available. [b] P. F. = primary face, S. F. = secondary face, E. W. = external wall, I. C. = internal cavity. [c] difference in NMR chemical shift of most affected CD proton between its free and bound states, $\Delta\delta = \delta_{bound} - \delta_{free}$. [d] calculated by NMR or ITC. [e] BOC = N-tert-butoxycarbonyl. [f] M = Co, Ni, Zn. [g] An = anthracene group.

Table 2. Summary of reported CD-octahedral metal cluster adducts studied in solution by NMR.

CD	{M_6} cluster	CD-Cluster adduct[a]	binding site[b]	Most affected H	Δδ (ppm)[c]	Binding constant $K_{1:1}$ (10^3 M^{-1})[d]	Ref.
α-CD	$[Re_6S_8(CN)_6]^{4-}$	Cluster@2CD	S. F.	H3	+0.15	0.27	41
	$[Re_6Se_8(CN)_6]^{4-}$	CD•POM	S. F.	H3	+0.15	0.030	41
	$[Re_6Te_8(CN)_6]^{4-}$	2CD•POM	E. W.	-	0	0	41
β-CD	$[Re_6S_8(CN)_6]^{4-}$	Cluster@2CD	S. F.	H3	+0.30	0.64	41
	$[Re_6Se_8(CN)_6]^{4-}$	Cluster@2CD	S. F.	H3	+0.45	0.78	41
	$[Re_6Te_8(CN)_6]^{4-}$	Cluster@2CD	S. F.	H3	+0.15	0.084	41
γ-CD	$[Re_6S_8(CN)_6]^{4-}$	Cluster@2CD	S. F.	H3	+0.40	0.90	6
	$[Re_6Se_8(CN)_6]^{3-}$	Cluster@2CD	S. F.	H3	+0.2	225	49
	$[Re_6Se_8(CN)_6]^{4-}$	Cluster@2CD	S. F.	H3	+0.45	1.5	6
	$[Re_6Te_8(CN)_6]^{4-}$	Cluster@2CD	S. F.	H5	+0.35	38	6
	$[Re_6S_8(H_2O)_6]^{2+}$	Cluster@2CD	S. F.	-	0	-	62
	$[Nb_6Cl_{12}(H_2O)_6]^{2+}$	Cluster@2CD	E. W.	H1/H4	-0.08	2.2	1
	$[W_6Br_8Cl_6]^{2-}$	Cluster@2CD	S. F.	H3	+0.46	-	48
	$[W_6I_8Cl_6]^{2-}$	Cluster@2CD	S. F.	H3	+0.60	-	48
	$[Mo_6Br_8Cl_6]^{2-}$	Cluster@2CD	S. F.	H5	+0.40	-	63
	$[Mo_6I_8Cl_6]^{2-}$	Cluster@2CD	S. F.	H5	+0.60	-	63
	$[Mo_6Cl_{14}]^{2-}$	Cluster@2CD	S. F.	H3/H5	+0.04	-	50
	$[Ta_6Br_{12}(H_2O)_6]^{2+}$	Cluster@2CD	S. F.	H3	+0.60	150	28

a) From crystal structure. b) S. F. = secondary face, E. W. = external wall. c) difference in NMR chemical shift of most affected CD proton between its free and bound states, $\Delta\delta = \delta_{bound} - \delta_{free}$. d) calculated by NMR or ITC.

Table 3. Summary of reported CD-boron cluster adducts studied in solution by NMR.

CD	Boron cluster	CD-Cluster adduct[a]	binding site[b]	Most affected H	Δδ (ppm)[c]	Binding constant $K_{1:1}$ (10^3 M^{-1})[d]	Ref.
α-CD	$[B_{10}H_{10}]^{2-}$	Cluster@CD	S. F.	H3	+0.05	0.035	55
	$[B_{10}H_9NCCH_3]^-$	-	S. F.	H3	+0.06	0.034	53
	$[B_{12}H_{12}]^{2-}$	-	-	-	0	-	22
	$[B_{12}H_{11}SH]^{2-}$	-	-	-	0	-	22
	$[(1,2\text{-}C_2B_9H_{11})_2\text{-}3,3'\text{-}Co]^-$	-	S. F.	H3	+0.25	-	42

	$[(1,2\text{-}Me_2\text{-}1,2\text{-}C_2B_9H_9)_2\text{-}3,3'\text{-}Co]^-$	-	S. F.	H3	+0.10	-	[42]
	$[(8,8'\text{-}Cl_2\text{-}(1,2\text{-}C_2B_9H_{10})_2\text{-}3,3'\text{-}Co]^-$	-	S. F.	H3	+0.10	-	[42]
	$[(8\text{-}I\text{-}1,2\text{-}C_2B_9H_{10})(1',2'\text{-}C_2B_9H_{11})\text{-}3,3'\text{-}Co]^-$	-	S. F.	H3	+0.15	-	[42]
β-CD	$[B_{10}H_{10}]^{2-}$	Cluster@CD[e]	I. C.	H5	+0.19	0.11	[55]
	$[B_{10}H_9NCCH_3]^-$	-	P. F.	H5	+0.15	0.30	[53]
	$[B_{12}H_{12}]^{2-}$	-	-	-	0	-	[22]
	$[B_{12}H_{11}SH]^{2-}$	-	S. F.	H5	+0.32	-	[22]
	$[B_{12}I_{12}]^{2-}$	-	P. F.	H6	+0.15	-	[22]
	$[B_{12}I_{11}\text{-}NH_2C_6H_4\text{-}m\text{-}NO_2]^{1-}$	-	-	H3	+0.10	18	[64]
	$[B_{12}I_{11}\text{-}NH_2C_6H_4\text{-}p\text{-}NO_2]^{1-}$	Cluster@CD[e]	S. F./ I. C.	H3	-0.15	19	[64]
	$[B_{12}I_{11}\text{-}S_2C_6H2\text{-}N_2O\text{-}p\text{-}NO_2]^{1-}$	Cluster@CD[e]	S. F.	H1/H2	-0.10	270	[65]
	$[B_{12}I_{11}\text{-}S_2C_4H_8N\text{-}C_6H2\text{-}N_2O\text{-}p\text{-}NO_2]^{1-}$	-	-	H6	-0.15	260	[65]
	$[B_{12}Br_{12}]^{2-}$	-	S. F.	H3	+0.08	-	[22]
	$[(1,2\text{-}C_2B_9H_{11})_2\text{-}3,3'\text{-}Co]^-$	-	S. F.	H3	+0.20	26	[42]
	$[(1,2\text{-}Me_2\text{-}1,2\text{-}C_2B_9H_9)_2\text{-}3,3'\text{-}Co]^-$	-	S. F.	H3	+0.30	21	[42]
	$[(8,8'\text{-}Cl_2\text{-}(1,2\text{-}C_2B_9H_{10})_2\text{-}3,3'\text{-}Co]^-$	-	S. F.	H3	+0.27	19	[42]
	$[(8\text{-}I\text{-}1,2\text{-}C_2B_9H_{10})(1',2'\text{-}C_2B_9H_{11})\text{-}3,3'\text{-}Co]^-$	-	S. F.	H3	+0.25	24	[42]
γ-CD	$[B_{10}H_{10}]^{2-}$	Cluster@CD[e]	I. C.	H5	+0.19	0.060	[55]
	$[B_{10}H_9NCCH_3]^-$	-	P. F.	H5	+0.18	0.72	[53]
	$[B_{12}H_{12}]^{2-}$	Cluster@CD[e]	S. F.	H5	+0.15	2.0	[22]
	$[B_{12}H_{11}SH]^{2-}$	Cluster@CD[e]	S. F.	H5	+0.32	7.8	[22]
	$[B_{12}Cl_{12}]^{2-}$	Cluster@CD[e]	S. F.	H3	+0.35	17	[22]
	$[B_{12}Br_{12}]^{2-}$	Cluster@2CD	S. F.	H5	+0.70	960	[22]
	$[B_{12}I_{12}]^{2-}$	Cluster@CD[e]	S. F.	H1	+0.10	67	[22]
	$[B_{12}H_{11}OH]^{2-}$	-	S. F.	H5	+0.10	0.62	[22]
	$[B_{12}H_{11}NH_3]^{2-}$	-	S. F.	H3	+0.05	1.7	[22]
	$[B_{12}H_{11}N(CH_2CH_2CH_3)_3]^{2-}$	-	P. F.	H6	+0.05	1.1	[22]
	$[B_{12}H_{11}O(CH_2)_4C(NH_2)CO_2H]^{2-}$	-	S. F.	H5	+0.20	-	[22]
	$[B_{12}I_{11}\text{-}NH_2C_6H_4\text{-}m\text{-}NO_2]^{1-}$	-	-	H5	+0.20	9.6	[64]
	$[B_{12}I_{11}\text{-}NH_2C_6H_4\text{-}p\text{-}NO_2]^{1-}$	-	-	H5	+0.15	7.6	[64]
	$[B_{12}I_{11}\text{-}NH_2C_6H_4\text{-}m\text{-}NO_2]^{1-}$	-	-	H6	+0.20	150	[65]
	$[B_{12}I_{11}\text{-}NH_2C_6H_4\text{-}p\text{-}NO_2]^{1-}$	-	-	H6	+0.15	590	[65]
	$[(1,2\text{-}C_2B_9H_{11})_2\text{-}3,3'\text{-}Co]^-$	-	P. F.	H6	+0.10	191	[42]

[(1,2-Me_2-1,2-$C_2B_9H_9)_2$-3,3'-Co]$^-$	-	S. F.	H3	+0.10	300	[42]
[(8,8'-Cl_2-(1,2-$C_2B_9H_{10})_2$-3,3'-Co]$^-$	-	S. F.	H3	+0.15	3600	[42]
[(8-I-1,2-$C_2B_9H_{10}$)(1',2'-$C_2B_9H_{11}$)-3,3'-Co]$^-$	-	S. F.	H3	+0.15	1300	[42]

[a] From crystal structure when available. [b] P. F. = primary face, S. F. = secondary face, I. C. = internal cavity. [c] difference in NMR chemical shift of most affected CD proton between its free and bound states, $\Delta\delta = \delta_{bound} - \delta_{free}$. [d] calculated by NMR or ITC. [e] From DFT calculation.

4. Relaxation and line broadening

Supramolecular contact may induce line broadening due to dipolar coupling between neighboring nuclear spins, and linewidths could be used as a probe to assess the strength of these interactions and the interatomic distances. In presence of paramagnetic atoms, the effect should even be amplified since the dominant NMR relaxation mechanisms are connected to the coupling of the strong magnetic moment of the unpaired electron with the adjacent nuclear magnetic moment. Examples of NMR studies involving paramagnetic species include reduced POMs and oxidized octahedral clusters.[49,54] Dramatic line broadening of NMR signals of the CD has been observed upon host-guest complexation, particularly those present in the inner sites (H3 and H5). Furthermore, relaxation studies showed significant decreases of relaxation rates T_1 and T_2 for these specific protons up to two-order of magnitude.[49] Interestingly, longitudinal relaxation T_1 was found to discriminate interacting protons better than the transverse relaxation T_2.

5. DOSY and 2D NMR tools to track aggregation and self-assembly

Diffusion Ordered SpectroscopY (DOSY) and Nuclear Overhauser Effect SpectroscopY (NOESY) or Rotating frame Overhauser Effect SpectroscopY (ROESY) are the most used 2D

NMR techniques to study the interaction of CD with organic, inorganic and hybrid guests. DOSY is the 2D version of pulsed field gradient (PFG) NMR measurement, used to determine the self-diffusivity of dissolved species. Thus, DOSY experiment correlates the chemical shift with the diffusion coefficient in the second dimension. This technique can allow differentiation between free and aggregated CD to other species or between them, and thus provide information about binding and exchange in CD-based supramolecular systems. As an example, the ^{1}H DOSY experiment revealed the host-guest complex formation between the Lindqvist-type functionalized hexavanadate $[V_6O_{13}((OCH_2)_3C\text{-}NO_2)_2]^{2-}$ and γ-CD.[59] The diffusion coefficient of the free hybrid POM in 2 mM D_2O drops from around 450 to 300 $\mu m^2/s$ when complexed with γ-CD, as a clear indication of the POM encapsulation process within the macrocycle. The diffusion coefficient of the free CD also decreased in the presence of POM, but only slightly, as the volume/size of the complex is dominated by that of CD. Nonetheless, the diffusion coefficient of hybrid POM is not perfectly aligned with that of the host molecule, indicating dynamic dissociation in solution. DOSY has thus proved an efficient technique for quantitatively studying chemical equilibria and exchange processes in CD-based hybrids with inorganic nanoclusters.[25,28]

For example, the formation of aggregates between γ-CD and Dawson-type POM $[P_2W_{18}O_{62}]^{6-}$ has been well demonstrated by ^{1}H and ^{31}P DOSY NMR, providing simultaneous access to the self-diffusion coefficient of γ-CD and that of the POM species, respectively.[15] The DOSY investigation, graphically shown in Fig. 8 reveals that the self-diffusion coefficients of the interacting substrates decrease significantly in the POM/γ-CD mixture that underline the formation of stable aggregates in solution. Interestingly, the *D* value of both interacting components reaches together the same minimum value at $D = 210\ \mu m^2/s$ observed for the composition range close to the 1:2 ratio ($\frac{POM}{POM+CD} = 0.33$). This result highlights that stable aggregates are formed provoking

large changes of self-diffusion coefficients of each component in the presence of large excess of the corresponding partner (see Fig. 8c). These DOSY NMR data corroborate nicely the analysis given by Stoddart et al. from SAXS/WAXS measurements carried out on aqueous solution containing the Keggin-type anion and γ-CD.[10] However, it is interesting to note that structural analysis by XRD (Fig. 8d) reveals that POM and CDs assemble through weak interactions highlighted by minimal variations in NMR chemical shifts (^{1}H, ^{183}W, and ^{31}P), while DOSY or SAXS/WAXS studies demonstrate that these hydrophilic species form stable aggregates in aqueous solution. This demonstrates the high sensitivity of the DOSY technique to supramolecular interaction.

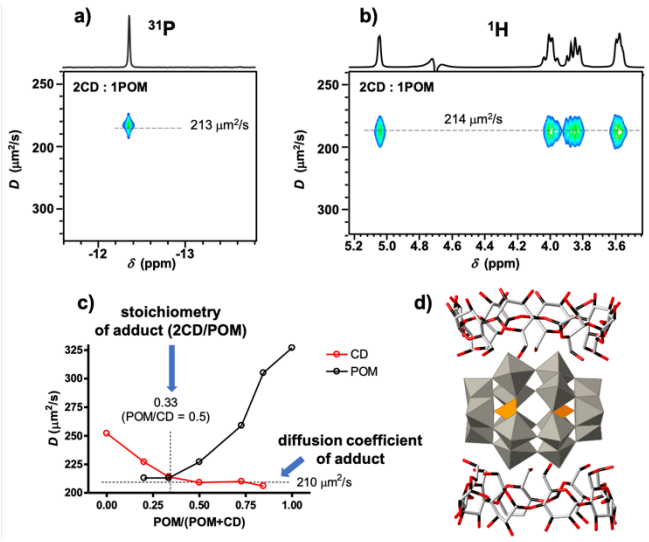

Fig. 8. 2D DOSY (a) ^{31}P and (b) ^{1}H spectra of a mixture of 2:1 γ-CD (3 mM): Dawson POM $[P_2W_{18}O_{62}]^{6-}$ (1.5 mM) revealing common diffusion coefficient at ca. 214 µm²/s. (c) Diffusion coefficients of the host (CD) and the guest (POM) measured by ^{1}H and ^{31}P DOSY as a function of POM fraction in POM-CD system. The two curves cross at POM/CD ratio of 0.5 corresponding to the stoichiometry of (d) the sandwich adduct evidenced by single crystal XRD. Adapted from reference.[15]

NOE-based experiments such as NOESY and ROESY are techniques of choice for studying non-covalent interactions in supramolecular systems involving cavitand molecules such as CDs. Such NMR methodologies based on "through space" interactions (or dipolar coupling) allow insight into which parts of a guest molecule are in spatial proximity to the hosting unit. ROESY is generally preferred to NOESY for the study of nanoscopic assemblies built with CD, as it enables to probe longer distances up to 5 Å and provides positive ROE signal for macromolecules and large chemical complexes. The sign of the NOE/ROE signals is an important parameter for differentiating other dynamic phenomena such as spin diffusion and exchange process, which lead to negative cross-peaks like the diagonal signals. Fig. 9 shows an example of application of ROESY experiment to the CD/$[B_{10}H_{10}]^{2-}$ systems.[55] For a 1:1 mixture of α-CD/$[B_{10}H_{10}]^{2-}$, the interactions between equatorial protons of the boron cluster He, with H3 and H5 internal protons of the α-CD are revealed through the occurrence of cross NOE peaks. For β-CD, the cross ROE peaks between the unresolved resonances of H5/H6 of the CD and both Ha and He of $[B_{10}H_{10}]^{2-}$indicate interactions between hydrogen atoms of the boron cluster and the CD. These results are fully consistent with the DFT-optimized structures of the adducts showing partially embedded cluster through the secondary face of α-CD and fully encapsulated cluster within the β-CD cavity. ROESY NMR technique has been employed successfully to probe the host-guest contacts through space occurring in solution between β-CD and Lindqvist-type hybrid hexavanadates.[59] Strong correlations were generally observed between the organic part of $[V_6O_{13}((OCH_2)_3C\text{-}R)_2]^{2-}$ derivatives, R = CH_2OH, CH_2CH_3, NO_2, and internal protons of the CD (mostly H3 and H5) fairly consistent with the host-guest structures observed in the solid-state. Recent examples of zirconium oxoclusters have also been reported.[66]

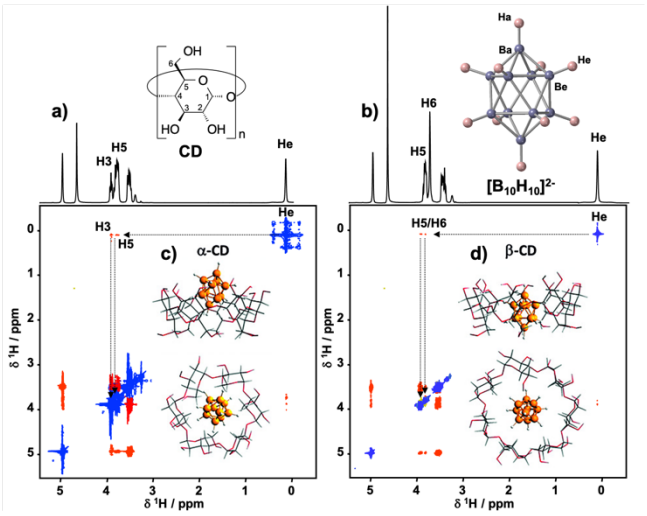

Fig. 9. 1D and 2D ^{1}H-^{1}H{^{11}B} ROESY NMR spectra in D_2O of a 1:1 mixture of (a) α-CD/$[B_{10}H_{10}]^{2-}$ and (b) β-CD/$[B_{10}H_{10}]^{2-}$. (c) and (d) the corresponding optimized DFT structures of the CD-cluster adducts. Adapted from reference.[55]

6. Use of guest NMR probes

When available other NMR nuclei than ^{1}H and ^{13}C of the host can be used to probe the supramolecular interaction between the CD and the inorganic guest. These NMR nuclei should then be present in the cluster part of the hybrid assembly, providing additional characterization from the guest's point of view. For example, ^{31}P NMR is used to follow the Dawson-type POM in the ternary system γ-CD:$[P_2W_{18}O_{62}]^{6-}$:$[Mo_{154}O_{462}H_{14}(H_2O)_{70}]^{14-}$.[30] In the binary system γ-CD: $[P_2W_{18}O_{62}]^{6-}$, the characteristic signal of the POM appeared similar to that of the free species at -12.3 ppm as an indication of labile dynamic {1:1} complex (Fig. 10). Introducing the giant blue wheel $\{Mo_{154}\}$ had led to resolved three additional signals assigned to POM@POM assembly with one and two capping CDs, {1:1:1} and {2:1:1}, respectively (Fig. 10). Such a frozen three-component assembly is made possible by the CD binding ability, which enables to bring two anionic species closer together. Indeed, no interaction could be observed in the absence of CD.

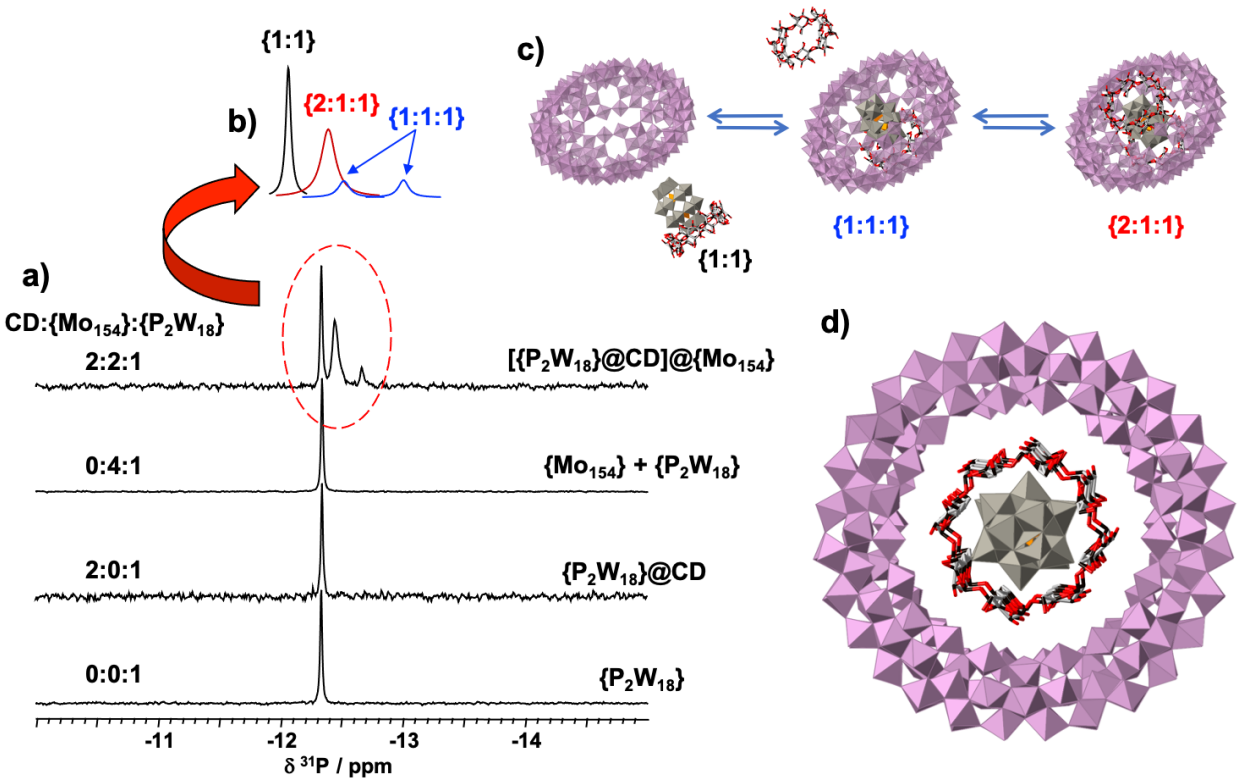

Fig. 10. (a) ^{31}P NMR spectrum in D_2O of Dawson POM $[P_2W_{18}O_{62}]^{6-}$ in the presence of γ-CD and the molybdenum blue wheel $[Mo_{154}O_{462}H_{14}(H_2O)_{70}]^{14-}$ compared to the spectra in the absence of one of them or both of them. The spectrum in the ternary system can be decomposed into (b) three components corresponding to the labile {1:1} CD:{P_2W_{18}}, and the ternary complexes {1:1:1} and {2:1:1} in the CD:{P_2W_{18}}:{Mo_{154}} system in (c) equilibrium in solution. The crystallographic structure of the {2:1:1} adduct (d) is consistent with a "host in host" hierarchical POM@CD@POM structure. Adapted from reference.[30]

In labile dynamically systems, ^{31}P NMR could not sense efficiently the host-guest interaction between the POM and the CD when the phosphorus is located in the internal pocket of the POM. The nucleus is in somehow shielded by the surrounding metal atoms, which protect the heteroatom from interaction with the surrounding environment. This is the case of the Dawson-type POM shown in Fig. 10 when exposed to CDs. However, external nuclei at the surface of the POM, such as ^{183}W NMR, should exhibit higher sensitivity towards supramolecular interaction at their surface. Fig. 11 shows the effect of presence of α–, β–, and γ-CD on the ^{183}W NMR of $[PW_{12}O_{40}]^{3-}$.[51]

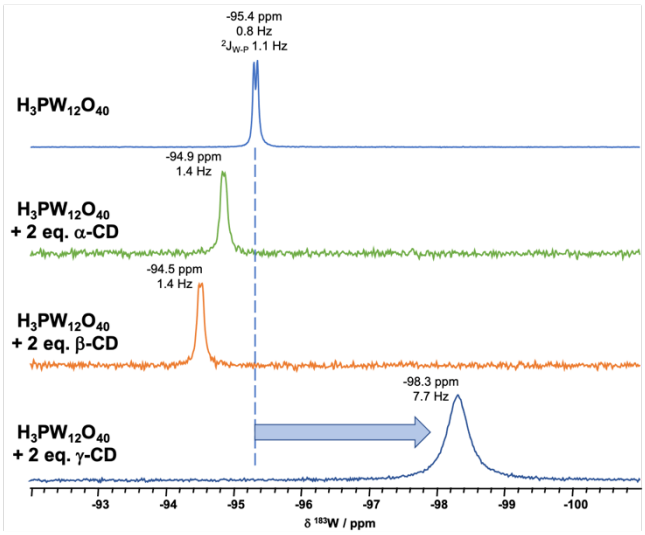

Fig. 11. ^{183}W NMR spectra in D_2O of 7.5 mM Keggin-type POM $[PW_{12}O_{40}]^{3-}$ in the absence and presence of 2 equivalents of α–, β–, and γ-CD. Adapted from reference.[51]

The Keggin POM $[PW_{12}O_{40}]^{3-}$ is characterized by a single sharp ^{183}W signal at –95.4 ppm corresponding to the 12 W equivalent nuclei of the POM structure (Fig. 11). This signal is actually a doublet due to the scalar coupling with the neighboring P heteroatom ($^2J_{W-P}$ = 1.1 Hz). With the addition of two equivalents γ-CD, this signal broadens and shifts toward high fields of about 3 ppm. These effects clearly indicate the formation of the inclusion complex with a very strong association, which provides a significant shielding on the W nuclei. The line broadening of the ^{183}W signal recalls that of the H3 proton of the CD (see Fig. 5) resulting from a strong host–guest contact. This interaction can therefore be tracked from the host side by ^{1}H NMR or the guest side by ^{183}W NMR. Furthermore, these effects are not observed with the other smaller CDs (Fig. 11), confirming the unique behavior of γ-CD highlighted by the formation of the inclusion complex. These effects are only moderately perceived by ^{31}P NMR, with a maximum variation of 0.4 ppm (from -14.3 to -14.7 ppm),[51] while ^{183}W NMR recorded a difference of ca. 3 ppm, as the outer metal centers are more exposed to interaction with CD than the inner heteroatom.

The metal transition octahedral clusters can also contain interesting active NMR nuclei. For instance, the ½-I nucleus ^{77}Se (7.63% natural abundance) has been used to study the interaction of the selenide rhenium cluster $[Re_6Se_8(CN)_6]^{4-}$ with γ-CD.[6] Fig. 12 shows the NMR titration of 24 mM solution by increasing the amount of the CD progressively up to 16 equivalents. A single signal is observed shifting progressively from δ = -389 ppm to the limiting value of -392.6 ppm. This indicates a fast exchange regime between the different cluster-based species, that is, solvated or embedded within γ-CD. The line broadening observed at intermediate CD equivalents (ca. 0.5 to 2) is indicative of formation of 1:1 intermediate labile complex. Similar behavior is observed in ^{1}H NMR titration of the same system shown in Fig. 2a, where the most affected H3 resonance experienced major line broadening at intermediate cluster equivalents. Job plots shown in Fig. 13 confirm the formation of the predominant 2:1 CD:Cluster type complex in aqueous solution as in the XRD structure.[6]

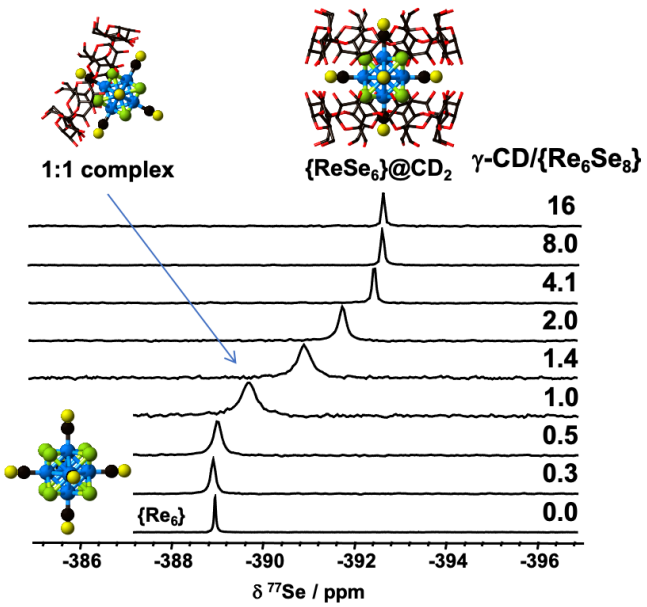

Fig. 12. ^{77}Se NMR titration of 24 mM $[Re_6Se_8(CN)_6]^{4-}$ in D_2O by γ-CD. Adapted from references.[36]

Job plot allows determining the stoichiometry of the adducts in solution, and can be applied either on the host or the guest. By plotting the product of the molar fraction of the host (CD) or the guest (cluster) in the mixture by the difference between observed chemical shift of the host (H3) or the guest (^{77}Se) in presence and absence of the cluster or the CD as a function of the molar fraction in the host or the guest, respectively, maxima indicate the stoichiometry. Job's plots drawn in Fig. 13 both give consistent results with the formation of 2:1 adduct.

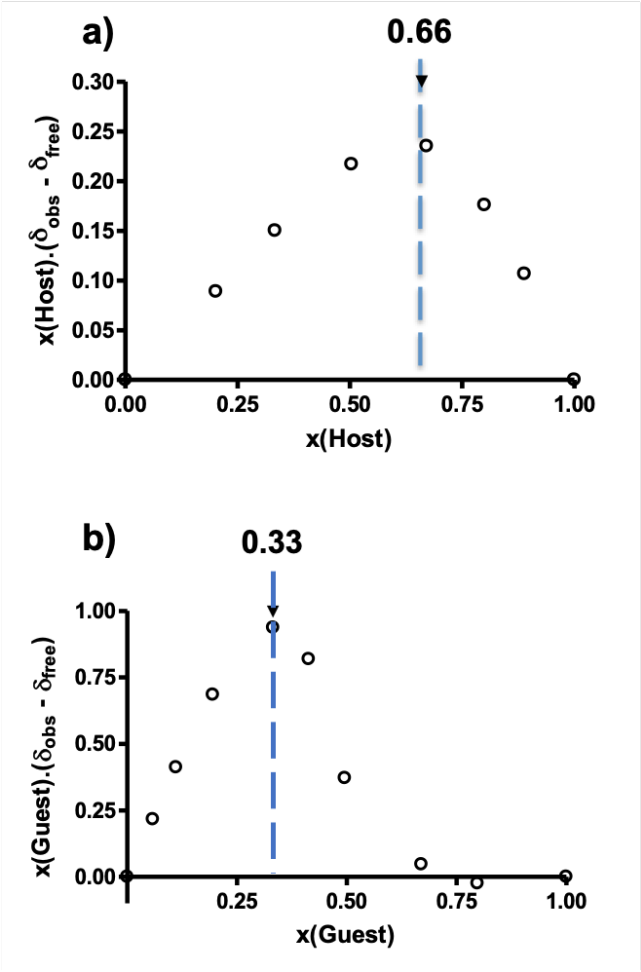

Fig. 13. Job plots obtained from NMR titration of (a) the host by the guest, or (b) the guest by the host in the host-guest system γ-CD:$[Re_6Se_8(CN)_6]^{4-}$, by using ^{1}H NMR signal H3 of γ-CD in (a) (spectra shown in Fig. 2a), or ^{77}Se NMR signal of the cluster in (b) (spectra shown in Fig. 12).

7. Concluding remarks and outlook

Over the past decade, significant progress has been made in the development of host-guest assemblies based on CDs and inorganic molecules, and this area of research continues to attract growing interest. Understanding the phenomena at play in solution in these systems, and characterizing them in their original environment, is essential for the search of new, more elaborate and complex supramolecular functional materials. NMR has proven to be a versatile, flexible and easy-to-implement technique for probing the weak interactions between these macrocycles and inorganic cluster molecules such as POMs, octahedral metal-atom clusters or boron clusters. Qualitative and quantitative information can be extracted by measuring the strength of mutual interaction, identifying binding sites, and studying chemical equilibria and molecular exchange.

Future research should focus on a better understanding of the role of water in host-guest complexation driven by solvent effect. NMR nuclei such as ^{1}H, ^{2}H, and ^{17}O would be excellent probes for identifying local interaction sites and monitoring dynamic behavior. Of particular interest, relaxation (T_2 and linewidth) and diffusion (DOSY) experiments could provide valuable information. Variable-temperature NMR experiments can also shed light on molecular motions. Finally, the gradual change in the nature of the medium from water to organic solvents (*e.g.*, DMSO) may also bring insight on the proton exchange process involving the hydroxyl groups in CD.

Nevertheless, with the ever-increasing complexity of these systems, the limits of the technique could be rapidly reached as of the size of the aggregates increases and the viscosity of the native medium decreases, as in hydrogels and supramolecular polymers. The restriction of molecular motion is the main drawback of high-resolution NMR spectroscopy. In this case, other

techniques more suited to semi-fluids and soft matter systems, such as cryo-TEM, DLS, SAXS, SANS, and solid-state NMR, can take over.

Conflicts of interest

The authors declare no competing financial interest.

Acknowledgments

This work was supported by the Paris Ile-de-France Region – DIM "Respore", and a public grant overseen by the French National Research Agency as part of the ''Investissements d'Avenir'' program (Labex Charm3at, ANR-11-LABX-0039-grant). We thank the former and present members of our team (Anton A. Ivanov, Mhamad Aly Moussawi, Yao Sa, Zeinab El Hajj, Ibrahima Bamba & Manal Diab) who performed the experiments and for spirited discussions for developing excellence in NMR practice.

References

1 A. A. Ivanov, T. N. Pozmogova, A. O. Solovieva, T. S. Frolova, O. I. Sinitsyna, O. V. Lundovskaya, A. R. Tsygankova, M. Haouas, D. Landy, E. Benassi, L. V. Shestopalova, C. Falaise, E. Cadot, M. A. Shestopalov, P. A. Abramov and M. N. Sokolov, *Chem.-Eur. J.*, 2020, **26**, 7479–7485.

2 Y.-M. Zhang, Q.-Y. Xu and Y. Liu, *Sci. Chin.-Chem.*, 2019, **62**, 549–560.

3 K. Kirakci, M. A. Shestopalov and K. Lang, *Coord. Chem. Rev.*, 2023, **481**, 215048.

4 J. Lee, S.-S. Lee, S. Lee and H. B. Oh, *Molecules*, 2020, **25**, 4048.

5 Y. Li, Y. Su, Z. Li and Y. Chen, *Polymers*, 2022, **14**, 4855.

6 A. A. Ivanov, C. Falaise, P. A. Abramov, M. A. Shestopalov, K. Kirakci, K. Lang, M. A. Moussawi, M. N. Sokolov, N. G. Naumov, S. Floquet, D. Landy, M. Haouas, K. A. Brylev, Y. V. Mironov, Y. Molard, S. Cordier and E. Cadot, *Chem.-Eur. J.*, 2018, **24**, 13467–13478.

7 K. Li, K.-L. Zhu, L.-P. Cui and J.-J. Chen, *Dalton Trans.*, , DOI:10.1039/d3dt00105a.

8 L. Ni, H. Li, H. Xu, C. Shen, R. Liu, J. Xie, F. Zhang, C. Chen, H. Zhao, T. Zuo and G. Diao, *ACS Appl. Mater. Interfaces*, 2019, **11**, 38708–38718.

9 W. Qi, C. Ma, Y. Yan and J. Huang, *Curr. Opin. Colloid Interface Sci.*, 2021, **56**, 101526.

10 Y. Chen, S. Sun, D. Lu, Y. Shi and Y. Yao, *Chin. Chem. Lett.*, 2019, **30**, 37–43.

11 L.-J. Xu, C.-M. Wang, K. Yu, C.-X. Wang and B.-B. Zhou, *Coord. Chem. Rev.*, 2023, **481**, 215044.

12 A. A. Kuznetsova, V. V. Volchek, V. V. Yanshole, A. D. Fedorenko, N. B. Kompankov, V. V. Kokovkin, A. L. Gushchin, P. A. Abramov and M. N. Sokolov, *Inorg. Chem.*, 2022, **61**, 14560–14567.

13 M.-N. Shen, X.-W. Lin, J. Luo, W.-Z. Li, Y.-Y. Ye and X.-Q. Wang, *Mol. Syst. Des. Eng.*, 2022, **7**, 1570–1587.

14 Z. Y. Wei, Z. K. Wu, S. Ru, L. B. Ni and W. Wei, *Chem. J. Chin. Univ.-Chin.*, 2022, **43**, 20210665.

15 D. Prochowicz, A. Kornowicz and J. Lewinski, *Chem. Rev.*, 2017, **117**, 13461–13501.

16 J. M. Cameron, G. Guillemot, T. Galambos, S. S. Amin, E. Hampson, K. Mall Haidaraly, G. N. Newton and G. Izzet, *Chem. Soc. Rev.*, 2022, **51**, 293–328.

17 W. Guan, G. Wang, B. Li and L. Wu, *Coord. Chem. Rev.*, 2023, **481**, 215039.

18 W. Guan, G. Wang, J. Ding, B. Li and L. Wu, *Chem. Commun.*, 2019, **55**, 10788–10791.

19 G. Izzet, M. Ménand, B. Matt, S. Renaudineau, L.-M. Chamoreau, M. Sollogoub and A. Proust, *Angew. Chem. Int. Ed.*, 2012, **51**, 487–490.

20 B. Li, L. Xuan and L. Wu, *Macromol. Rapid Commun.*, 2022, 2200019.

21 B. Zhang, W. Guan, S. Zhang, B. Li and L. Wu, *Chem. Commun.*, 2016, **52**, 5308–5311.

22 K. I. Assaf, M. S. Ural, F. Pan, T. Georgiev, S. Simova, K. Rissanen, D. Gabel and W. M. Nau, *Angew. Chem.-Int. Edit.*, 2015, **54**, 6852–6856.

23 Y. Wu, R. Shi, Y.-L. Wu, J. M. Holcroft, Z. Liu, M. Frasconi, M. R. Wasielewski, H. Li and J. F. Stoddart, *J. Am. Chem. Soc.*, 2015, **137**, 4111–4118.

24 K. I. Assaf and W. M. Nau, *Angew. Chem. Int. Ed.*, 2018, **57**, 13968–13981.

25 S. Yao, C. Falaise, A. A. Ivanov, N. Leclerc, M. Hohenschutz, M. Haouas, D. Landy, M. A. Shestopalov, P. Bauduin and E. Cadot, *Inorg. Chem. Front.*, 2021, **8**, 12–25.

549 26 C. Falaise, M. A. Moussawi, S. Floquet, P. A. Abramov, M. N. Sokolov, M. Haouas and
550 E. Cadot, *J. Am. Chem. Soc.*, 2018, **140**, 11198–11201.

551 27 N. Leclerc, M. Haouas, C. Falaise, S. Al Bacha, L. Assaud and E. Cadot, *Molecules*, 2021,
552 **26**, 5126.

553 28 M. A. Moussawi, N. Leclerc-Laronze, S. Floquet, P. A. Abramov, M. N. Sokolov, S.
554 Cordier, A. Ponchel, E. Monflier, H. Bricout, D. Landy, M. Haouas, J. Marrot and E. Cadot, *J.*
555 *Am. Chem. Soc.*, 2017, **139**, 12793–12803.

556 29 C. Falaise, S. Khlifi, P. Bauduin, P. Schmid, W. Shepard, A. A. Ivanov, M. N. Sokolov,
557 M. A. Shestopalov, P. A. Abramov, S. Cordier, J. Marrot, M. Haouas and E. Cadot, *Angew. Chem.-*
558 *Int. Edit.*, 2021, **60**, 14146–14153.

559 30 M. A. Moussawi, M. Haouas, S. Floquet, W. E. Shepard, P. A. Abramov, M. N. Sokolov,
560 V. P. Fedin, S. Cordier, A. Ponchel, E. Monflier, J. Marrot and E. Cadot, *J. Am. Chem. Soc.*, 2017,
561 **139**, 14376–14379.

562 31 X.-Y. Hu and D.-S. Guo, *Angew. Chem. Int. Ed.*, 2022, e202204979.

563 32 D.-L. Long and L. Cronin, in *Recent Highlights I*, eds. C. D. Hubbard and R. VanEldik,
564 2021, vol. 78, pp. 227–267.

565 33 J. Luo, X. Sun, J.-F. Yin, P. Yin and T. Liu, *Giant*, 2020, **2**, 100013.

566 34 S. Passadis, T. A. Kabanos, Y.-F. Song and H. N. Miras, *Inorganics*, 2018, **6**, 71.

567 35 M. Stuckart, N. V. Izarova, J. van Leusen, A. Smekhova, C. Schmitz-Antoniak, H.
568 Bamberger, J. van Slageren, B. Santiago-Schübel and P. Kögerler, *Chem. Eur. J.*, 2018, **24**,
569 17767–17778.

570 36 Z. Zhu, M. Wei, B. Li and L. Wu, *Dalton Trans.*, 2021, **50**, 5080–5098.

571 37 E. Bertaut and D. Landy, *Beilstein J. Org. Chem.*, 2014, **10**, 2630–2641.

572 38 Y. Fan, S. Lu and J. Cao, *Int. J. Mass Spectrom.*, 2019, **435**, 163–167.

573 39 P. Su, A. J. Smith, J. Warneke and J. Laskin, *J. Am. Soc. Mass Spectrom.*, 2019, **30**, 1934–
574 1945.

575 40 Y. Yuguchi, *Trend. Glycosci. Glycotechnol.*, 2009, **21**, 1–12.

576 41 A. A. Ivanov, C. Falaise, K. Laouer, F. Hache, P. Changenet, Y. V. Mironov, D. Landy, Y.
577 Molard, S. Cordier, M. A. Shestopalov, M. Haouas and E. Cadot, *Inorg. Chem.*, 2019, **58**, 13184–
578 13194.

579 42 K. I. Assaf, B. Begaj, A. Frank, M. Nilam, A. S. Mougharbel, U. Kortz, J. Nekvinda, B.
580 Grüner, D. Gabel and W. M. Nau, *J. Org. Chem.*, 2019, **84**, 11790–11798.

581 43 B. Chankvetadze, *Chem. Soc. Rev.*, 2004, **33**, 337–347.

44 H. Dodziuk, W. Kozminski and A. Ejchart, *Chirality*, 2004, **16**, 90–105.

45 M. Haouas, C. Falaise, C. Martineau-Corcos and E. Cadot, *Crystals*, 2018, **8**, 457.

46 H. J. Schneider, F. Hacket, V. Rudiger and H. Ikeda, *Chem. Rev.*, 1998, **98**, 1755–1785.

47 A. A. Ivanov, C. Falaise, A. A. Shmakova, N. Leclerc, S. Cordier, Y. Molard, Y. V. Mironov, M. A. Shestopalov, P. A. Abramov, M. N. Sokolov, M. Haouas and E. Cadot, *Inorg. Chem.*, 2020, **59**, 11396–11406.

48 C. Falaise, A. A. Ivanov, Y. Molard, M. A. Cortes, M. A. Shestopalov, M. Haouas, E. Cadot and S. Cordier, *Mater. Horizons*, 2020, **7**, 2399–2406.

49 A. A. Ivanov, C. Falaise, D. Landy, M. Haouas, Y. V. Mironov, M. A. Shestopalov and E. Cadot, *Chem. Commun.*, 2019, **55**, 9951–9954.

50 A. A. Ivanov, P. A. Abramov, M. Haouas, Y. Molard, S. Cordier, C. Falaise, E. Cadot and M. A. Shestopalov, *Inorganics*, 2023, **11**, 77.

51 S. Yao, C. Falaise, N. Leclerc, C. Roch-Marchal, M. Haouas and E. Cadot, *Inorg. Chem.*, 2022, **61**, 4193–4203.

52 K. Hirose, in *Analytical Methods in Supramolecular Chemistry*, Wiley-VCH, Germany, Ed: C. A. Schalley. Chapter 2, 2012, vol. 1, pp. 27–66.

53 Z. El Hajj, S. Calancea, M. Haouas, D. Landy, D. Naoufal and S. Floquet, *J. Clus. Sci.*, 2023, 10.1007/s10876-023-02468–x.

54 S. Yao, C. Falaise, S. Khlifi, N. Leclerc, M. Haouas, D. Landy and E. Cadot, *Inorg. Chem.*, 2021, **60**, 7433–7441.

55 M. Diab, S. Floquet, M. Haouas, P. A. Abramov, X. Lopez, D. Landy, A. Damond, C. Falaise, V. Guerineau, D. Touboul, D. Naoufal and E. Cadot, *Eur. J. Inorg. Chem.*, 2019, 3373–3382.

56 P. Yang, W. Zhao, A. Shkurenko, Y. Belmabkhout, M. Eddaoudi, X. Dong, H. N. Alshareef and N. M. Khashab, *J. Am. Chem. Soc.*, 2019, **141**, 1847–1851.

57 P. Yang, B. Atshankiti and N. M. Khashab, *Crystengcomm*, 2020, **22**, 2889–2894.

58 S. Khlifi, J. Marrot, M. Haouas, W. E. Shepard, C. Falaise and E. Cadot, *J. Am. Chem. Soc.*, 2022, **144**, 4469–4477.

59 I. F. Bamba, C. Falaise, J. Marrot, P. Atheba, G. Gbassi, D. Landy, W. Shepard, M. Haouas and E. Cadot, *Chem.-Eur. J.*, 2021, **27**, 15516–15527.

60 Z.-Q. Qi, M.-Y. Wang, J.-C. Shen, Y.-Z. Lan, Z.-G. Jiang and C.-H. Zhan, *Chem. Commun.*, 2022, **58**, 13616–13619.

61 Z.-G. Jiang, W.-T. Mao, D.-P. Huang, Y. Wang, X.-J. Wang and C.-H. Zhan, *Nanoscale*, 2020, **12**, 10166–10171.

62 P. A. Abramov, A. A. Ivanov, M. A. Shestopalov, M. A. Moussawi, E. Cadot, S. Floquet, M. Haouas and M. N. Sokolov, *J. Clust. Sci.*, 2018, **29**, 9–13.

63 A. A. Ivanov, M. Haouas, D. V. Evtushok, T. N. Pozmogova, T. S. Golubeva, Y. Molard, S. Cordier, C. Falaise, E. Cadot and M. A. Shestopalov, *Inorg. Chem.*, 2022, **61**, 4462−14469.

64 T. Marei, M. K. Al-Joumhawy, M. A. Alnajjar, W. M. Nau, K. Assaf and D. Gabel, *Chem. Commun.*, 2022, **58**, 2363–2366.

65 K. I. Assaf, O. Suckova, N. Al Danaf, V. von Glasenapp, D. Gabel and W. M. Nau, *Org. Lett.*, 2016, **18**, 932–935.

66 G. Hoyez, J. Rousseau, C. Rousseau, S. Saitzek, J. King, P. A. Szilagyi, C. Volkringer, T. Loiseau, F. Hapiot, E. Monflier and A. Ponchel, *Crystengcomm*, 2021, **23**, 2764–2772.